Title

Local calcium transients contribute to disappearance of pFAK, focal complex removal and deadhesion of neuronal growth cones and fibroblasts

Journal

Developmental Biology, 287(1)

ISSN

0012-1606

Authors

Conklin, M W
Lin, M S
Spitzer, Nicholas C

Publication Date

2005-11-01

Peer reviewed

Available online at www.sciencedirect.com
SCIENCE DIRECT
Developmental Biology 287 (2005) 201 – 212
DEVELOPMENTAL BIOLOGY
www.elsevier.com/locate/ydbio

Local calcium transients contribute to disappearance of pFAK, focal complex removal and deadhesion of neuronal growth cones and fibroblasts

Matthew W. Conklin, Margaret S. Lin, Nicholas C. Spitzer *

Neurobiology Section, Division of Biological Sciences, UCSD, La Jolla, CA 92093, USA
Center for Molecular Genetics, Division of Biological Sciences, UCSD, La Jolla, CA 92093, USA

Received for publication 30 April 2005, revised 19 August 2005, accepted 1 September 2005
Available online 3 October 2005

Abstract

Cell adhesion is crucial for migration of cells during development, and cell–substrate adhesion of motile cells is accomplished through the formation and removal of focal complexes that are sites of cell–substrate contact. Because Ca^{2+} signaling regulates the rate of axon outgrowth and growth cone turning, we investigated the potential role of Ca^{2+} in focal complex dynamics. We describe a novel class of localized, spontaneous transient elevations of cytosolic Ca^{2+} observed both in *Xenopus* neuronal growth cones and fibroblasts that are 2–6 μm in spatial extent and 2–4 s in duration. They are distributed throughout growth cone lamellipodia and at the periphery of fibroblast pseudopodia, which are regions of high motility. In both cell types, these Ca^{2+} transients lead to disappearance of phosphorylated focal adhesion kinase (pFAK) and deadhesion from the substrate as assessed by confocal and internal reflection microscopy, respectively. The loss of pFAK is inhibited by cyclosporin A, suggesting that these Ca^{2+} transients exert their effects via calcineurin. These results identify an intrinsic mechanism for local cell detachment that may be modulated by agents that regulate motility.

Keywords: Calcineurin; Calcium signaling; Confocal microscopy; Fibroblasts; Focal complexes; Focal adhesion kinase; Growth cones; Internal reflection microscopy

Introduction

Cell motility is a dynamic process that involves orchestration of cytoskeletal elements, molecular motors, membrane turnover, intracellular signaling, energy metabolism, and both the formation and removal of localized regions of adhesion to the extracellular matrix (ECM) (Lauffenburger and Horwitz, 1996; Geiger and Bershadsky, 2001). These subcellular regions, termed focal adhesion contacts, are the sites through which the traction force necessary for cellular movement is generated (Ingber, 2003). Neuronal motility is regulated in part by diffusible molecules extrinsic to the cell, such as Netrin or Slit acting as soluble or tethered guidance cues (Ming et al., 2002; Plump et al., 2002). These molecules bind specific receptors and initiate signaling pathways that modify the cytoskeleton or other components. Motility is also a function of intrinsic properties, governed in part by the formation and turnover of focal adhesion contacts. Adhesion is the result of clusters of membrane-spanning integrin receptors that link the extracellular matrix to the cytoskeleton, in conjunction with many other intracellular signaling and structural proteins that comprise the focal contact (Zemir and Geiger, 2001). Thus, these regions are positioned to initiate signaling cascades and are potentially regulated by second messengers such as Ca^{2+}.

Transient elevations in cytosolic Ca^{2+} are required for migration of neutrophils (Marks and Maxfield, 1990; Hendey and Maxfield, 1993), vascular smooth muscle cells (Scherberich et al., 2000), and neurons (Komuro and Rakic, 1996). Ca^{2+} transients have also been shown to have functions related to growth cone motility (Gu and Spitzer, 1995; Gomez and Spitzer, 1999; Zheng, 2000; Gomez et al., 2001; Tang et al., 2003). Two distinct classes of spontaneous Ca^{2+} transients occur in developing *Xenopus* spinal neurons at specific frequencies and spatial locations with distinct amplitudes and durations. Growth cone Ca^{2+} transients regulate axon extension

* Corresponding author. Neurobiology Section 0357, Division of Biological Sciences, University of California San Diego, 9500 Gilman Dr., La Jolla, CA 92093-0357, USA. Fax: +1 858 534 7309.
E-mail address: nspitzer@ucsd.edu (N.C. Spitzer).

0012-1606/$ - see front matter © 2005 Elsevier Inc. All rights reserved.
doi:10.1016/j.ydbio.2005.09.006

(Gu and Spitzer, 1995; Gomez and Spitzer, 1999), and filopodial Ca^{2+} transients contribute to growth cone turning (Gomez et al., 2001). Using rapid confocal imaging with fluo-4 AM, we have observed another class of Ca^{2+} transient, the localized lamellipodial transient (LLT) in growth cones and the localized fibroblast transient (LFT) in fibroblasts.

Small spontaneous elevations of intracellular Ca^{2+} analyzed in cardiac and skeletal muscle (sparks; Cheng et al., 1993; Conklin et al., 2000) have been reported in neurons. In nerve growth factor-differentiated PC12 cells, localized elevations of intracellular Ca^{2+} occur preferentially at neuritic branch points (Koizumi et al., 1999). Localized elevations of intracellular Ca^{2+} occur in the spines of hippocampal cells (Bonhoeffer and Yuste, 2002) and may contribute to spine motility. In astrocytoma cells, Ca^{2+} transients propagated throughout the cytoplasm appear to contribute to focal adhesion disassembly (Giannone et al., 2002). The effect of transient elevations of second messengers on focal complexes could be significant because integrins have no known catalytic activity, and thus, signaling at focal contacts must be carried out by other molecules. One such molecule is focal adhesion kinase (FAK), which is autophosphorylated in response to integrin–substrate binding (Calalb et al., 1995). This activation of FAK has been shown to lead to disassembly of focal adhesion contacts at a later time. Cells cultured from FAK knockout mice adhere strongly to the substrate but do not grow or extend processes, indicating a role of FAK in focal contact turnover (Ilic et al., 1995).

We have characterized properties of LLTs and analyzed their function in the context of motility. Using an antibody to the autophosphorylated form of FAK (pFAK), we find that immunoreactivity of growth cones of cultured neurons stained for focal contacts is inversely correlated with LLT frequency. We hypothesize that these Ca^{2+} transients contribute to focal contact turnover and ultimately the removal of pFAK immunoreactivity (pFAK-IR). We demonstrate that growth cones in which Ca^{2+} is uncaged deadhere from the substrate as assayed by interference reflection microscopy, indicating removal of these cellular spot welds. We show that deadhesion following an LLT is correlated with a localized void of focal complexes as assayed by pFAK-IR. Growth cones are motile in the absence of LLTs, however; thus, Ca^{2+} is not the only mechanism for focal contact removal. Similar results are observed for LFTs in fibroblasts. The effects of these transients are blocked by inhibition of calcineurin in both cell types. Ca^{2+} transients may be a common signaling mechanism for the removal of focal complexes and deadhesion, contributing to the array of processes that constitute motility.

Materials and methods

Cell culture

For cultures of neurons, *Xenopus laevis* embryos at the neural plate stage (Nieuwkoop and Faber stage 15) were transferred to a modified Ringer's solution (MR; in mM: 100 NaCl, 2 KCl, 1 $MgSO_4$, 2 $CaCl_2$, 5 HEPES, pH adjusted to 7.4 with HCl). The neural plate was dissected (Ribera and Spitzer, 1989) and placed in MR containing 1 mg/ml collagenase B (Boehringer-Mannheim, Indianapolis, IN) to enable removal of somites. The remaining tissue was transferred to a Ca^{2+}-free medium for 60 min for dissociation. Cells were then aspirated through a fine bore glass pipette and plated directly onto uncoated or coated Corning tissue culture dishes containing MR or osmotically balanced MR containing 0 mM Ca^{2+}, 10 mM Ca^{2+}, 30 mM Ca^{2+}, or 30 mM Ca^{2+} plus 100 nM BAPTA-AM. Culture dishes were coated with ECM molecules by exposure to saturating concentrations (50 μg/ml laminin, 250 μg/ml poly-D-lysine, 50 μg/ml fibronectin, 50 μg/ml vitronectin, 10 μg/ml tenascin; all from Sigma, St Louis MO) for 1 h followed by five washes with phosphate-buffered saline (PBS). Neurite extension begins at ~6 h in culture and growth cones migrated on all substrates tested, advancing in an irregular and saltatory manner. Growth cones were imaged and cultures were processed for immunocytochemistry at 8–24 h in vitro.

For cultures of fibroblasts, ventral mesoderm of stage 20 embryos was separated from the rest of the embryo and the associated endodermal layer was removed. The remaining tissue was dissected into explants ~200 μm in diameter and plated onto dishes precoated with 50 μg/ml laminin and bathed in MR. Fibroblasts migrate out of the explants. The most rapidly moving cells at the periphery were imaged at 17–24 h in culture before processing cultures for immunocytochemistry.

Calcium imaging

Spinal neurons and fibroblasts were loaded with Ca^{2+} indicator in a solution of MR containing 2 mM fluo-4 AM (Molecular Probes, Eugene OR), 0.1% DMSO, and 0.01% pluronic for 45–60 min at room temperature. Images of fluo-4 AM loaded cells were acquired using a Bio-Rad (Hercules CA) MRC-1024 confocal attachment on an Olympus BX-50WI upright microscope (Melville NY) with a 100× PlanApo N.A. = 1.0 infinity-corrected water-immersion objective. Cells were scanned by the 488 nm line produced by a krypton/argon laser attenuated to 3% intensity through neutral density filters, and emitted photons >515 nm were collected and digitized for analysis. 500 consecutive images consisting of 128 × 128 pixels were acquired at a calibrated rate of one image per 184 ms (5.4 Hz) with a pixel size of 0.2 μm. A single series of images was captured in 92 s, without photobleaching, morphological changes indicating photodamage, or differences in Ca^{2+} transient generation during subsequent imaging periods. Pharmacological susceptibilities of LLTs and LFTs were assessed by addition of drugs to the culture medium.

Analysis and statistics

Image stacks were imported into NIH Image 1.62 software (W. Rasband, NIH), and LLTs and LFTs were initially identified by eye when the image stack was animated. The following properties of individual transients were measured: peak fluorescence intensity ratio (F/F_o), time to peak fluorescence, and duration and diameter at baseline. Using the line-drawing tools, a region of interest was traced around LLTs and LFTs, and measurements of average pixel intensity within regions of interest were acquired. This measurement was repeated for each image in the stack, and the data were exported to SigmaPlot 5.0.1 (Jandel, Chicago IL) for analysis. These data were plotted against the calibrated rate of image acquisition to yield kinetic and fluorescence intensity ratio data. Spatial data were acquired directly using the plot profile tool of NIH Image with calibrated pixel size; the margins of cells were truncated by the surface plot rendering in some cases. Incidence data are the percentage of imaged cells that generated at least one LLT or LFT. The frequency data included imaging periods without transients and were thus calculated as the total number of transients divided by the total imaging time and expressed as transients per minute. Values are presented as mean ± SEM. An unpaired Student's t test at the $p < 0.05$ level was used to determine statistical significance unless otherwise indicated.

Immunocytochemistry

Neurons or fibroblasts were rinsed in Ca^{2+} and Mg^{2+}-free (CMF)-PBS, fixed in 4% paraformaldehyde at 20°C for 10 min, and blocked with 1% fish gelatin in CMF-PBS for 30 min. The antibody specific for the autopho-

sphorylated form of FAK (pFAK; rabbit anti-FAK [pY397] primary antibody, 1:300 with 0.1% Triton; Biosource International, Camarillo CA) was then incubated overnight at 4°C. After two washes in PBS for 10 min each, Alexa-Fluor-488 goat anti-rabbit IgG secondary antibody (1:300, Molecular Probes) was incubated for 1 h at RT followed by two washes in PBS for 10 min each. Kalman-averaged images of pFAK immunofluorescence were acquired on the confocal microscope using the 100× objective. All images were acquired under identical confocal settings, antibody concentrations, and image contrast. No signal was detected in the absence of primary antibody. RGDS or RGES peptide was applied 5 min before fixation. Tenascin borders were created by placing Sylgard strips at the bottom of the culture dish during coating using a mixture of tenascin and TRITC–dextran to visualize the border. TRITC–dextran alone did not alter pFAK-IR.

Interference reflection microscopy

Laminin-coated (1 μg/ml) thin glass (No. 0) coverslips containing stage 20 neural tube explants plated for 24 h were inverted and stuck to glass slides using double sided adhesive tape. Internal reflection microscopy (IRM) imaging (Singer et al., 1989; Drazba et al., 1997) was performed using a 100× UPlanFL N.A. = 1.3 oil-immersion infinity-corrected objective and Bio-Rad (Hercules CA) MRC-600 confocal attachment on an Olympus BX-50WI upright microscope (Melville, NY) with the primary dichroic mirror replaced by a 50/50 beamsplitter, the emission filter removed, and the confocal aperture fully opened. IRM takes advantage of the interference of reflected light waves (488-nm laser line). In an IRM image, regions of the plasma membrane in close apposition to the substrate appear dark due to destructive interference of the two reflected sets of light waves from the cell and coverslip, respectively. Regions of membrane further away appear bright due to constructive interference. Because of the high numerical aperture of the lens, interferences beyond zero-order and reflections caused by the upper cell membrane are absent from the images (Verschueren, 1985). IRM was used in conjunction with analysis of pFAK immunoreactivity in fixed cells to calibrate the relationship of membrane adhesion to focal complex localization. pFAK puncta were judged to be colocalized with IRM puncta when they overlapped by >50%. IRM was also used to assay cellular apposition to coverslips at a given instant in a living cell. To track dynamics of cell adhesion, we acquired three consecutive IRM images at 5-min intervals and subtracted one image from the previous image to generate IRM difference images that indicate the change in adhesion over that time period. The numerical values of pixels in the IRM difference images were sorted into bins and plotted as histograms.

Online supplemental material

The video from which Fig. 1D was taken is available on line. It illustrates the dynamics of LLT generation in the growth cone of a cultured embryonic *Xenopus* spinal neuron. Blue color represents the baseline fluorescence of the Ca^{2+} indicator fluo-4, and red represents 150% of this baseline fluorescence. Frames were captured at 5.4 Hz for a period of 92 s and displayed at 18.4 frames/s.

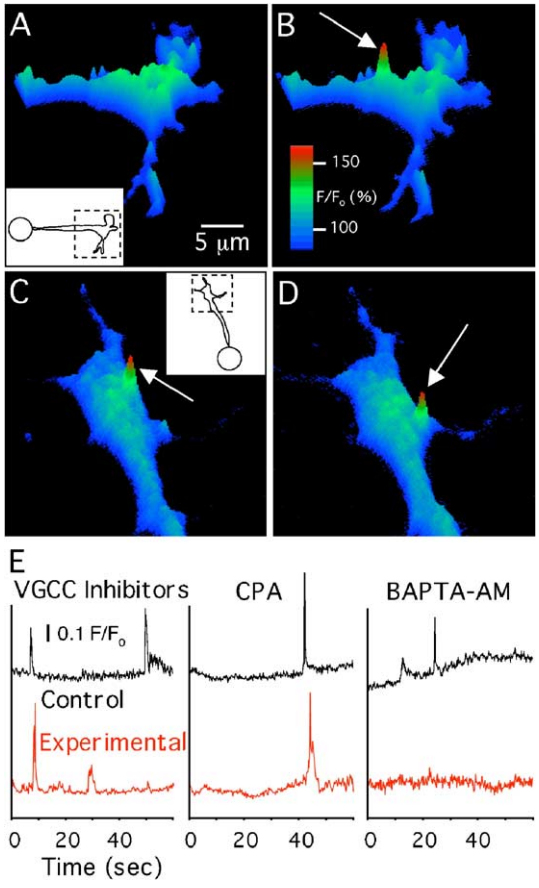

Fig. 1. Localized lamellipodial transients (LLTs) in migrating growth cones. (A, B) A spontaneous LLT in a *Xenopus* spinal neuron growth cone is shown in surface plots of two consecutive confocal images acquired 184 ms apart, before and during the LLT. Arrow indicates the LLT in panel B. Warmer colors are assigned to higher intensity values (*z*-axis) to highlight LLTs. The dashed box in the inset illustrates the imaged region of the cell. (C, D) In another growth cone, two non-consecutive surface plots demonstrate the generation of LLTs from two different sites. The video from which panel D was generated is available in Supplementary material online. Presentation is as for panels A, B. (E) Fluorescence intensity (*y*-axis) is plotted with respect to time for a region of interest encompassing a site of LLT generation during control periods (upper traces, black) and in the presence of either a combination of voltage-gated Ca^{2+} channel (VGCC) blockers (1 μM ω-conotoxin GVIA, 100 nM nifedipine, 50 nM ω-agatoxin IVA), or 10 μM CPA (cyclopiazonic acid), or 100 nM BAPTA-AM (lower traces, red) for periods ≥ 10 min. $n > 3$ trials for each experiment. LLTs are unaffected by Ca^{2+} channel blockers and CPA but are suppressed by BAPTA.

Results

Localized lamellipodial transients (LLTs) are spontaneous brief elevations in cytosolic Ca^{2+}

The description of small Ca^{2+} sparks and puffs in muscle, oocytes, neurons, and PC12 cells (Cheng et al., 1993; Yao et al., 1995; Koizumi et al., 1999) motivated a search for similar Ca^{2+} transients in neuronal growth cones. Cultured *Xenopus* spinal neurons loaded with fluo-4 AM and imaged at 5.4 Hz for brief periods revealed a class of Ca^{2+} elevations that we have designated local lamellipodial transients (LLTs). LLTs are spontaneous elevations in cytosolic Ca^{2+} (Figs. 1A, B). They occur at a frequency of 0.8 ± 0.1 min^{-1} in the total population of growth cones imaged and have an amplitude of 130 ± 1% of baseline fluorescence, a duration of 1.9 ± 0.2 s, a time to peak of 0.6 ± 0.1 s, and a diameter of 2.2 ± 0.1 μm (n = 52; tissue culture plastic substrate and 2 mM Ca^{2+} medium). They are observed in 51% of growth cones imaged for 92 s, but LLTs are not absent from half the population. Growth cones appear to cycle between periods of inactivity in which LLTs are absent, and periods of activity in which LLTs are present: lamellipodia in which no LLTs were observed during the first 92-s imaging period were observed to generate LLTs during later imaging periods. One to five LLT generation sites were observed in active growth cones during a single imaging period of 92 s (Figs. 1C, D; see Supplemental video), and a single site was seen to generate LLTs up to six times. In comparison to Ca^{2+}

spikes or growth cone transients (Gu and Spitzer, 1995; Gomez and Spitzer, 1999), LLTs are more frequent, smaller in spatial dimension, dimmer in fluorescence, with a more rapid time course. On the other hand, when compared to filopodial transients (Gomez et al., 2001), LLTs are less frequent, larger in size, lower in fluorescence intensity, and slower in rise and decay.

LLTs are abolished by the addition of 100 nM of the cell-permeant form of BAPTA to chelate intracellular Ca^{2+} (Fig. 1E; $n = 30$). However, these Ca^{2+} transients are not inhibited by a combination of pharmacological blockers that have previously been shown to be effective in selectively inhibiting voltage-gated Ca^{2+} channels in *Xenopus* spinal neurons (1 μM ω-conotoxin GVIA, 100 nM nifedipine, and 50 nM ω-agatoxin IVA; $n = 10$). These results make it unlikely that stretch-activated N-type Ca^{2+} channels (Calabrese et al., 2002) are involved in generating LLTs because these channels are blocked by ω-conotoxin GVIA. LLTs are also unaffected by 10 μM cyclopiazonic acid or 1 μM thapsigargin ($n = 10$), both of which block the Ca^{2+} ATPase of the endoplasmic reticulum, suggesting that release of Ca^{2+} from intracellular stores does not contribute to these events. The mean amplitude, duration, and diameter of LLTs observed following these pharmacological manipulations were not significantly different from the means during control conditions. LLTs are rapidly abolished by application of 10 mM Ni^{2+} or by removal of external Ca^{2+} ($n = 30$), consistent with generation by influx of Ca^{2+} across the plasma membrane through an as yet unidentified Ca^{2+} channel that appears not to be voltage-gated. However, thapsigargin-independent Ca^{2+} stores have been reported (Bian et al., 1991; Johnson and Chang, 2000), Ni^{2+} can block release of intracellular Ca^{2+} (Chakrabarti et al., 1995), and Ca^{2+}-free medium can deplete intracellular stores. Accordingly, definitive pharmacological resolution of the mechanism of generation of LLTs awaits the discovery of more selective inhibitors.

The incidence and frequency with which cells generate LLTs vary with the substrate on which the cells are plated but do not appear to depend on the concentration of extracellular Ca^{2+} from 2 to 30 mM (Fig. 2; $n \geq 30$ for each condition). LLTs were generated at the highest frequency on tissue culture plastic and at lower frequencies on extracellular matrix molecules fibronectin and vitronectin. However, their amplitude, duration, and diameter remained unchanged under these different conditions. LLTs were absent when grown on tenascin. The basis of the efficacy of tissue culture plastic is not known, but the coating on Corning "treated polystyrene" tissue culture dishes is an oxygenated form of polystyrene with random addition of hydroxyl, aldehyde, and carboxylic acid groups to the polymer that could enable integrin binding; alternatively, cells may secrete ECM molecules that coat the tissue culture plastic. We observed no change in their properties throughout early neuronal differentiation; all measured parameters were constant regardless of the age of neurons in culture from 8 to 24 h in vitro. Thus, LLTs appear to be unitary and stereotypic events with a distinct substrate dependence of initiation.

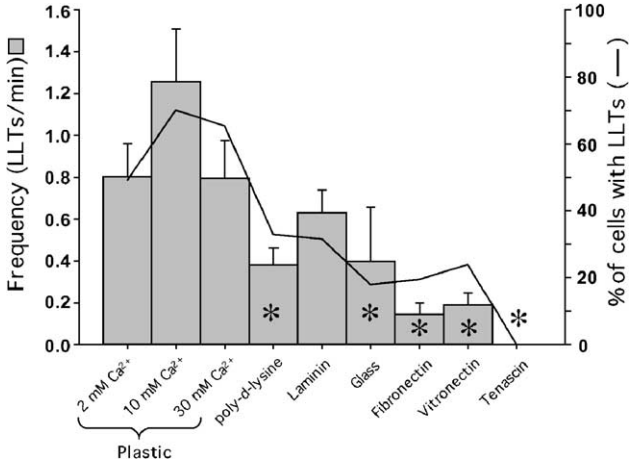

Fig. 2. Properties of LLTs. The frequency (bars) and incidence (line) of LLTs vary with the extracellular matrix substrate. The frequency of LLTs/min includes imaging periods without LLTs. The number of growth cones imaged is ≥30 in each condition. Asterisks denote statistically different from 2 mM Ca^{2+} (Student's t test, $p < 0.05$). Neurons were grown in 2 mM Ca^{2+} medium (MR) unless otherwise indicated.

Immunoreactivity of neuronal pFAK is punctate, increased by integrin activation, and decreased by Ca_i^{2+}

Growth cone Ca^{2+} transients determine the rate of axon outgrowth and filopodial Ca^{2+} transients control turning of the growth cone—both processes requiring cytoskeletal reorganization (Gu and Spitzer, 1995; Lautermilch and Spitzer, 2000; Gomez et al., 2001). We thus investigated whether cells generating LLTs also exhibit cytoskeletal rearrangements to perform a cellular function related to motility. Since LLTs are local events, we hypothesized that their effects will also be local and examined the localized region of the cell responsible for adhesion. Focal contacts are found in all cells at sites where they make localized contact with the extracellular matrix (ECM). They are continuously being formed and removed in moving cells (Izzard and Lochner, 1980; Davies et al., 1993) and contain integrin receptors that bind ECM molecules and are linked to the cytoskeleton. Thus, they are well positioned to initiate signaling cascades upon binding ECM and activate (among other components) focal adhesion kinase (FAK), a tyrosine kinase that is known to promote the turnover of focal contacts (Ilic et al., 1995). In growth cones, integrin receptors bind ECM molecules followed by increased integrin receptor avidity until a cluster is formed. Concomitantly, cytoskeletal and signaling molecules bound to integrin receptors are also clustered resulting in a primitive focal contact termed a focal complex that can be considered a functional cellular spot weld. During this maturation process, FAK becomes autophosphorylated (pFAK; Kornberg et al., 1992; Schaller et al., 1994) and is now capable of phosphorylating tyrosines on other molecules. The functions of several cytoskeletal proteins are regulated by pFAK binding and/or phosphorylation by pFAK (Schaller, 2001). Because the incidence and frequency of LLTs vary with the ECM substrate on which the cells are plated, we hypothesize that LLTs generate elevations of cytosolic Ca^{2+} at the focal complex

which combine with FAK phosphorylation to result in the localized collapse of the spot weld and cell detachment from the ECM.

Cultured spinal neurons immunocytochemically stained for the pY397 moiety of pFAK demonstrate punctate staining throughout the growth cone (Figs. 3A–D). pFAK is a useful marker for focal complexes because autophosphorylation of FAK does not take place until the complex has matured (Kornberg et al., 1992), thereby reducing staining from molecules trafficking to the complex. Previous work demonstrated that activation of integrins with RGDS peptide stimulates acute elevations of cytoplasmic Ca^{2+} that are blocked by antibodies to β1 integrin (Gomez et al., 2001); these Ca^{2+} elevations mimic LLTs. To test the hypothesis that pFAK expression is regulated by integrins in the absence of Ca^{2+} influx, we examined the effect of RGDS peptide in the presence of 10 mM Ni^{2+} to block Ca^{2+} entry during LLTs. This concentration of Ni^{2+} blocks all voltage-gated Ca^{2+} channels in these neurons. RGDS plus Ni^{2+} produces an increase in pFAK staining in less than 5 min (Fig. 3E) that is not produced by the non-integrin binding RGES peptide. Thus, integrin activation stimulates focal complex formation and pFAK-IR in the absence of LLTs as hypothesized above.

We find that the density of pFAK staining is also affected by the conditions that influence the incidence of LLTs. Cells grown and imaged in the absence of extracellular Ca^{2+} or grown on poor LLT-generating ECM substrates contain a high level of pFAK staining, while conditions that generate higher frequencies of LLTs reduce pFAK staining. Growth in 30 mM external Ca^{2+} decreases pFAK-IR when compared to staining following growth in 0 mM Ca^{2+}, and this effect is reversed by BAPTA-AM, suggesting that signaling via elevations of intracellular Ca^{2+} regulates pFAK-IR (Figs. 4A–D). BAPTA-AM suppresses Ca^{2+} transients but does not affect the steady level of cytosolic Ca^{2+} in growth cones (Gu and Spitzer, 1995). This regulation is also evident in cultures grown in 2 mM Ca^{2+}, where neurons grown on tenascin (a non-LLT-generating ECM substrate) exhibit significantly higher pFAK-IR when compared to neighboring neurons grown in the same dish on tissue culture plastic (where LLTs are generated; 206 ± 36%, $n = 12$ for each condition; Fig. 4E). These data raise the possibility that LLTs contribute to the removal of cellular spot welds containing pFAK.

Parallel pathways to focal complex removal

Formation of focal complexes is regulated by integrin binding (Zemir and Geiger, 2001; Fig. 3E). Removal of focal complexes is regulated at least partially by pFAK (Ilic et al., 1995; Sieg et al., 1999; Ren et al., 2000). pFAK immunoreactivity (Figs. 3, 4) of fixed cells represents a snapshot at a given time of the difference between two separate processes, the formation and removal of focal complexes, each of which occur at a separate rate (Geiger and Bershadsky, 2001). Tyrosine phosphorylation of a neuronal L-type Ca^{2+} channel results in an increase in its open probability at resting, hyperpolarized potentials (Bence-Hanulec et al., 2000), and pFAK is responsible for an integrin-stimulated increase in L-type Ca^{2+} current in smooth muscle (Wu et al., 2001). Accordingly, we asked if Ca^{2+} influx via LLTs is stimulated by pFAK. Genestein does not affect LLT production at 1 mM—more than tenfold the concentration that is effective in blocking the phosphorylation of FAK and substrate adhesion (Kyle et al., 1997; Danker et al., 1998). The absence of an effect of genestein on LLT generation suggests that binding of integrins to ECM substrate elicits LLTs and activates FAK in parallel. The removal of focal complexes is then the result of the combined effects of LLTs and pFAK.

Internal reflection microscopy identifies growth cone adhesion to substrate

To test the hypothesis that the parallel activation of FAK and LLTs leads to loss of adhesion via removal of focal complexes, we used interference reflection microscopy (IRM) to examine focal complexes more directly. IRM takes advantage of the

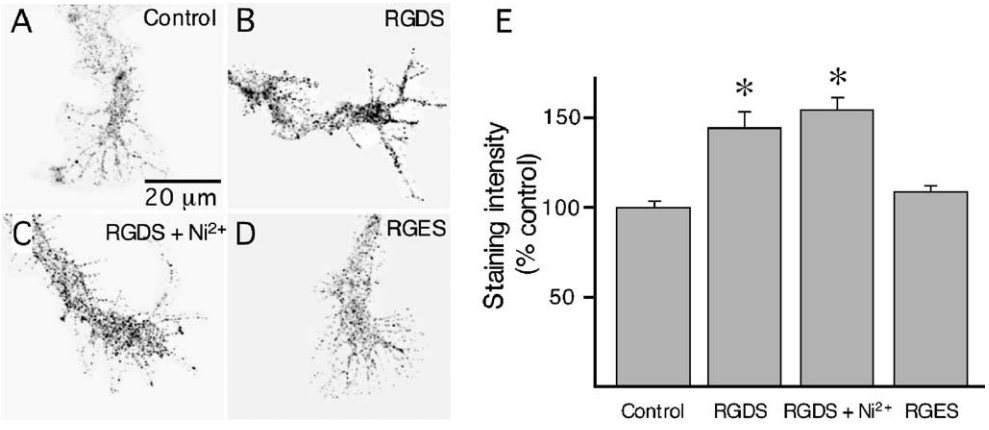

Fig. 3. Regulation of pFAK immunofluorescence by integrin activation. (A) pFAK staining in control (2 mM Ca^{2+} medium). (B) +RGDS (1 mM). (C) +RGDS + 10 mM Ni^{2+}. (D) + RGES (1 mM). Neurons were grown on tissue culture plastic. Images are inverted (immunofluorescence is black). (E) The mean pFAK staining intensity is significantly increased in cells incubated with the integrin activating peptide RGDS for 5 min prior to fixation. This effect is not blocked by the prior addition of Ni^{2+} to prevent LLTs, nor is it achieved by the non-integrin activating peptide RGES. $n \geq 10$ growth cones for each condition. Asterisks denote statistically different from 2 mM Ca^{2+} ($p < 0.05$) and not different from each other.

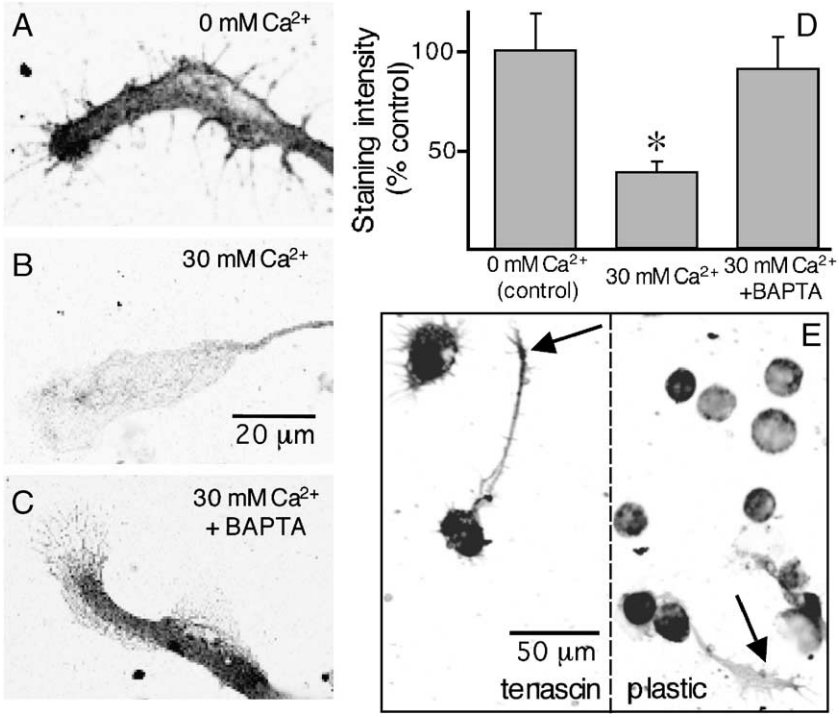

Fig. 4. pFAK staining is influenced by factors that reduce LLT frequency. (A) Growth cones of cells grown in 0 mM Ca^{2+} are more densely stained than those of cells grown in 2 mM Ca^{2+} (Fig. 3A). (B, C) Light staining in the presence of osmotically balanced 30 mM extracellular Ca^{2+} is converted to dense staining by exposure to 100 nM BAPTA-AM. (D) The mean pFAK staining intensity is decreased significantly when cells are grown in the presence of extracellular Ca^{2+}; this effect is blocked by addition of BAPTA to suppress elevation of intracellular Ca^{2+} (Gu and Spitzer, 1995). $n > 20$ growth cones for each condition. Asterisk denotes statistically different from 0 mM Ca^{2+} and 30 mM Ca^{2+} plus BAPTA ($p < 0.05$). (E) pFAK staining is more intense in cells grown in 2 mM Ca^{2+} on tenascin where LLTs are absent than on tissue culture plastic where LLTs are present; arrows identify two growth cones on these different substrates in the same culture, ~200 μm apart.

interference of reflected light waves when the distances between the plasma membrane and the glass coverslip on which the cell is plated are on the order of scale of the wavelength of the light. Membrane in close apposition to the substrate appears dark due to destructive interference of the two reflected sets of light waves from the cell and coverslip, while regions of membrane further away appear bright due to constructive interference. In growth cones of sensory neurons grown on fibronectin, immunostaining of paxillin, zyxin, and β1 integrin are localized with focal contacts (Gomez et al., 1996). In keratocytes, increased immunofluorescence of β_1-integrin and talin corresponds to dark regions in an IRM image, indicating their localization to regions of close cell–substrate contact (Lee and Jacobson, 1997). Although this technique does not measure adhesion directly, it is often used to assess adhesion, and the close apposition between membrane and substrate has been found to be associated with focal contacts (Singer et al., 1989). Focal contacts, in turn, are sites of high force attachment to the substrate (Balaban et al., 2001). Comparison of pFAK-IR with IRM of the same growth cone reveals that 75% of puncta corresponding to pFAK staining (colored red) show overlap with dark puncta in the IRM (destructive interference, colored green) that resemble focal complexes (Fig. 5). The correlation is not one-to-one, and the presence of more focal complexes than pFAK puncta suggests that rates of disappearance of pFAK-IR and the adhesions viewed with IRM are not identical. Nevertheless, IRM is useful because it allows examination of cellular adhesion.

Growth cone deadhesion and focal complex removal are regulated by LLTs

To examine dynamic changes in cell adhesion in living growth cones induced by changes in Ca_i^{2+}, we acquired three consecutive IRM images at 5-min intervals and uncaged Ca^{2+} from NP-EGTA (Gomez and Spitzer, 1999) between the second and the third. Subtraction of the 2nd and 3rd images from those previous to them generated two IRM difference images (Figs. 6A–C). This interval was determined by measuring the minimal length of time needed to observe a significant change between image intensity histograms pre- and post-UV Ca^{2+} uncaging. The change was not statistically significant at post-UV uncaging intervals of 1 or 3 min but became significant at intervals of 5 min or greater (Wilcoxon test, $p < 0.05$; $n = 3$ for each time interval). These images indicate the change in adhesion over this time period. Qualitatively, the images were pseudocolored to represent changes in adhesion (Figs. 6B,C). Quantitatively, numerical pixel values in the IRM difference images were plotted as histograms (Fig. 6D). We used this procedure to track changes in adhesion before and after a 100-ms UV-uncaging pulse to photorelease Ca^{2+} throughout growth cones. This pulse generates a Ca^{2+} transient comparable to an LLT in amplitude and duration although not spatial extent (not shown). Comparison of the two IRM difference images pre- and post-UV uncaging demonstrates net deadhesion from the substrate. In pseudocolored images, this is represented as an increase in

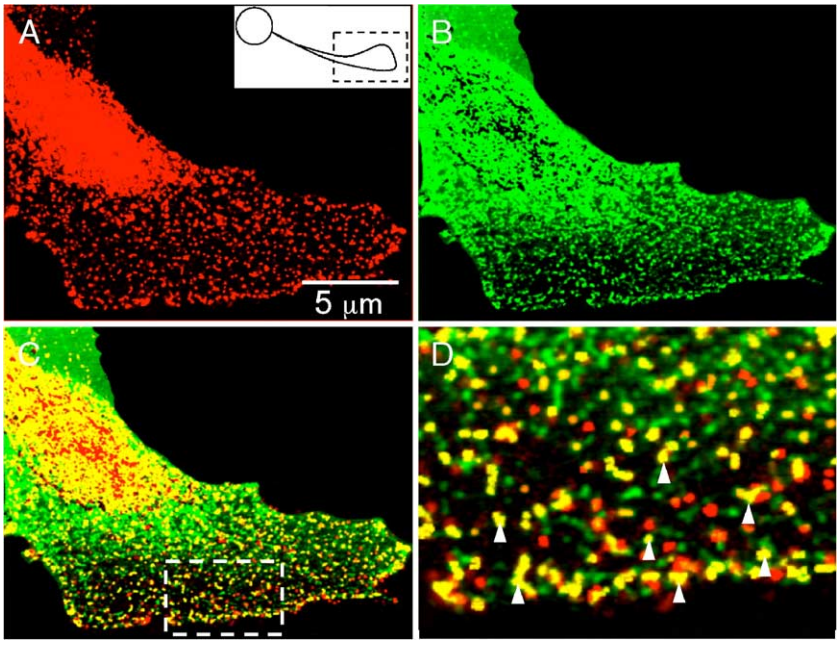

Fig. 5. pFAK immunoreactivity colocalization with focal complexes in lamellipodia. (A, B) Images of the growth cone of a cultured neuron fixed and stained for pFAK-IR (red) and examined using IRM (green). Inset in panel A shows growth cone region of interest. Merged images at intermediate (C) and high magnification (D, boxed region in panel C) reveal that most of the red spots representing focal complexes are in register with green spots (yielding yellow), indicating close cell–substrate contact in the distal regions of the veil of the lamellipodium (examples indicated by white arrowheads).

cooler (blue and purple) color and a decrease in warmer (red) color in the IRM difference image following uncaging. Additionally, comparison of histograms of the IRM difference image values reveals a significant increase in the numbers of pixels representative of deadhesion (Wilcoxon test; $n = 3$, $p < 0.05$). UV stimulation in the absence of NP-EGTA had no detectable effect on the IRM image assessed in this manner ($n = 4$), and uncaging Ca^{2+} in cells loaded with BAPTA (100 nM BAPTA-AM for 20 min) prevented the change in adhesion ($n = 5$). Therefore, a transient elevation in Ca^{2+} causes the cell to deadhere from the substrate, raising the possibility that this is associated with removal of focal complexes.

To test the role of LLTs in removal of focal complexes, we imaged growth cones to identify the production of LLTs and fixed the cultures after 5 min to examine pFAK immunoreactivity. As hypothesized, the region of the growth cone in which an LLT was generated shows a reduction in number of pFAK-IR puncta (Figs. 7A, B). pFAK-IR, quantified in the region defined by the full width at half maximum of the LLT, fell to 49 ± 4% of control areas ($n = 6$). Control area values were calculated as the average of the mean pixel intensity from three separate regions of equal area, adjacent to the site of LLT generation. Growth cones in which no LLTs were observed during the 92-s imaging period exhibited an even distribution of punctate pFAK-IR, and arbitrarily selected areas equivalent to those in which LLTs were generated were not different from controls (102 ± 1%; Figs. 7C, D, $n = 6$). The cycling of growth cones between active and inactive states noted above, in which LLTs are present or absent, suggests that a substantial number of growth cones that were inactive during the 92 s of imaging were inactive for longer periods.

Fibroblasts also generate localized elevations of intracellular Ca^{2+}

Most studies of focal complexes have been performed in non-excitable cells that are rapidly migrating (Izzard and Lochner, 1980; Davies et al., 1993). Accordingly, we tested the hypothesis that the contribution of local Ca^{2+} transients to loss of focal complexes is not specific to neuronal growth cones but is observed in fibroblasts as well. We find that *Xenopus* fibroblasts generate both global and local Ca^{2+} transients. Global transients, occurring throughout the cytoplasm, are generated at a frequency of 2 h^{-1}, have an amplitude of 148 ± 5% of baseline fluorescence, and are 26 ± 2 s in duration in 7% of cells imaged for 1 h ($n = 37$). In contrast, localized fibroblast transients (LFTs, Fig. 8A) occur more frequently at 0.25 ± 0.03 min^{-1} and have an amplitude of 133 ± 5% of baseline fluorescence; they are 4 ± 1 s in duration, have a time to peak of 1.0 ± 0.3 s, and a diameter of 6.0 ± 2.0 μm in 12% of cells imaged for 92 s ($n = 16$, 50 μg/ml laminin substrate and 2 mM Ca^{2+} medium). As in growth cones, fibroblasts appear to cycle between periods of activity and inactivity in which LFTs are present and absent; fibroblasts in which no LFTs were observed during the first 92-s imaging period were observed to generate LFTs during later imaging periods. One to three LFT generation sites were observed in single fibroblasts during a single imaging period of 92 s, and a single site was observed to generate LFTs up to three times. In 15 out of 16 instances, the LFT was generated at the periphery of the fibroblast, the most motile portion of the cell. Transients are abolished when cells are loaded with BAPTA (100 nM BAPTA-AM for 30 min; Fig. 8B). Unlike LLTs in neuronal growth cones, both classes of fibroblast

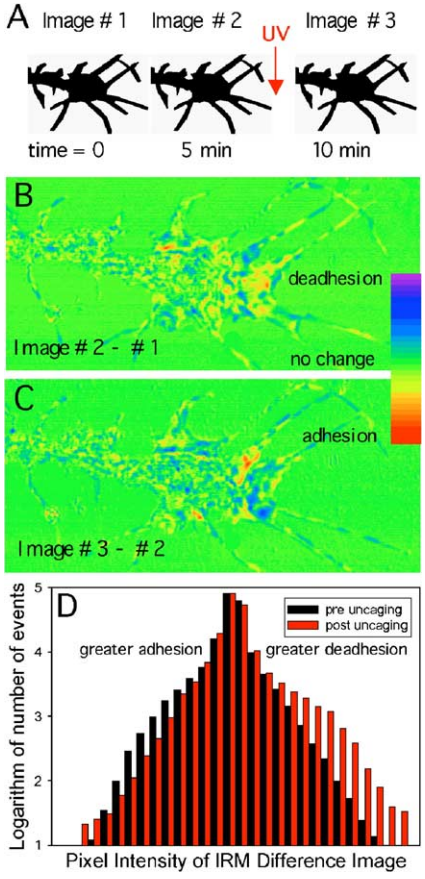

Fig. 6. UV uncaging of Ca^{2+} stimulates change in net growth cone–substrate proximity. (A) Cartoon illustrating the experimental protocol shows 3 IRM images acquired 5 min apart, with Ca^{2+} uncaging between the 2nd and 3rd images. (B) Subtraction of image 1 from image 2 illustrates pseudocolored baseline changes before uncaging. (C) Subtraction of image 2 from image 3 demonstrates changes following Ca^{2+} uncaging. (D) Histogram of pixel values from these two difference images indicates that there is less adhesion (left side) and greater deadhesion (right side) following Ca^{2+} uncaging. The difference is significant at $p < 0.05$ (Wilcoxon test).

transients are suppressed by the application of 200 mM tetracaine or 100 mM ryanodine (Fig. 8B), demonstrating a role for ryanodine receptor channels in the generation of these signals.

Fibroblast deadhesion and focal complex removal are regulated by LFTs

Because LFTs resemble LLTs but appear to involve release of Ca^{2+} from intracellular Ca^{2+} stores, we determined whether Ca^{2+} transients in fibroblasts have a function similar to that observed in neurons. Cells were imaged for LFTs, fixed 5 min after LFT generation, and imaged with IRM (Figs. 9A, B). The region of the cell that generated the LFT corresponds to a bright region in the IRM image, indicating that this portion of the cell is not in contact with the substrate. Using the full width at half maximum of the LFT as a diameter, mean intensity measurements within the LFT area of the IRM image are 40 ± 3% brighter in intensity when compared to control regions ($n = 5$; significant at 0.05, Wilcoxon test).

In corresponding experiments, fibroblasts were imaged for LFTs, fixed, and processed for pFAK immunoreactivity (Figs. 9C, D). Fibroblasts immunocytochemically stained for pFAK exhibit punctate focal complexes at the edges and vertices of cells where the cytoskeletal tension is highest (Ingber, 2003), as well as staining in the interior portions of the cell. Regions of cells in which LFTs were generated corresponded to local areas in which pFAK staining was reduced to 60 ± 3% of control areas ($n = 7$). This result parallels observations from neurons and indicates that localized elevations in intracellular Ca^{2+} have a localized effect on adhesion in fibroblasts as well.

The actions of LFTs and LLTs are blocked by inhibition of calcineurin

Calcineurin has been shown to have key roles in several aspects of cell motility. Growth cone Ca^{2+} transients that are larger in amplitude and broader in spatial extent than LLTs inhibit growth cone migration by engaging the Ca^{2+}-dependent phosphatase calcineurin (Lautermilch and Spitzer, 2000). Local inactivation of calcineurin causes filopodial retraction (Chang et al., 1995). Calcineurin also plays a role in regulation of flagellar motility (Tash et al., 1988) and neutrophil migration on vitronectin (Hendey et al., 1992; Lawson and Maxfield, 1995). We investigated the role of calcineurin in mediating the actions of LFTs and LLTs by examining the effect of cyclosporin A, a well-characterized and specific inhibitor of calcineurin.

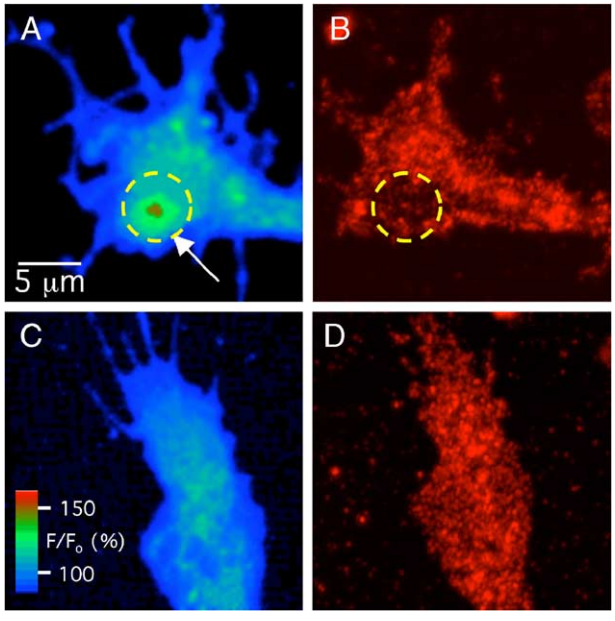

Fig. 7. The site of LLT generation coincides with low pFAK immunoreactivity. (A) Fluo-4 fluorescence image of a growth cone generating an LLT (arrow). (B) pFAK immunoreactivity of the same cell 5 min following the incidence of the LLT shows reduced staining in the region of the growth cone where the LLT occurred (yellow dashed circle). This result was observed in 6 of 6 neuronal growth cones that were fixed and stained for pFAK following the observation of an LLT during Ca^{2+} imaging. (C) Fluo-4 image of a growth cone not generating an LLT during the period of imaging. (D) There are no regions of distinctively low intensity pFAK immunoreactivity in the growth cone. Results similar to panels C and D were obtained from 6 of 6 growth cones.

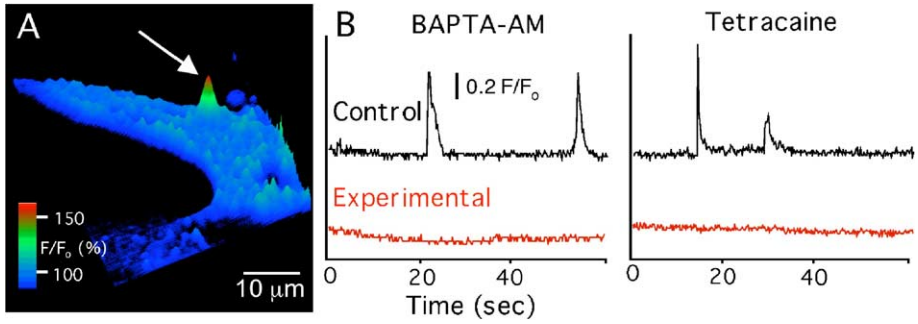

Fig. 8. Localized Ca^{2+} transients are generated in fibroblasts. (A) Surface plot of fluo-4 fluorescence in a fibroblast generating a localized transient (arrow). (B) Graphs of fluorescence intensity vs. time for a region of interest encompassing a site of LFT generation during a control period (upper traces, black) and in the presence of 100 nM BAPTA-AM or 200 mM tetracaine (lower traces, red). $n > 3$ trials for each experiment.

Following 1-h incubation in 10 nM cyclosporin A, a concentration shown to suppress the effect of growth cone Ca^{2+} transients (Lautermilch and Spitzer, 2000), localized Ca^{2+} transients were imaged in fibroblasts and growth cones loaded with fluo 4-AM. The incidence of LFTs and LLTs was similar to those of controls (16% vs. 12% for LFTs and 38% vs. 51% for LLTs), but frequencies were significantly reduced (0.10 ± 0.01 min^{-1} vs. 0.25 ± 0.03 min^{-1} for LFTs ($n = 90$) and 0.24 ± 0.09 min^{-1} vs. 0.8 ± 0.1 min^{-1} for LLTs (n ± 8); $p < 0.05$). LFTs had amplitudes 157 ± 7% of baseline fluorescence and durations of 2.9 ± 0.5 s ($n = 5$), comparable to 130 ± 1% and 1.9 ± 0.2 s in controls. LLTs had amplitudes 124 ± 7% of baseline and durations of 1.0 s ($n = 2$), similar to 133 ± 5% and 4 ± 1 s in controls. To determine the effects of these transients, cells were fixed within 3–5 min following imaging and processed for immunocytochemistry. pFAK-IR in the domains of the LFTs and LLTs was not different from that in areas of the cells in which no transients were observed, in contrast with the reductions noted in the absence of cyclosporin A (Fig. 10; n = 7). These results suggest that LFTs and LLTs activate calcineurin as part of a signal transduction pathway by which focal complexes are disassembled.

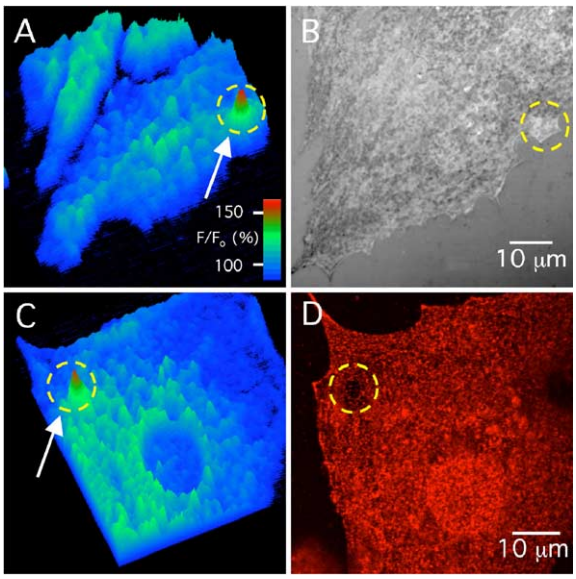

Fig. 9. The site of LFT generation coincides with low adhesion and low pFAK immunoreactivity. (A) Surface plot of fluo-4 fluorescence in three fibroblasts, one of which generated a localized transient during the period of imaging (arrow). (B) The culture was fixed 5 min after imaging the LFT, and the same fibroblasts were analyzed by IRM. The location of the LFT (yellow dashed circle) coincides with brighter intensity in the IRM image. Similar results were obtained from 5 of 5 cells. (C) Surface plot of fluo-4 fluorescence in another fibroblast, which generated an LFT. (D) The culture was fixed 5 min after imaging the LFT and stained for pFAK. The site of LFT generation corresponds to a localized reduction in pFAK immunoreactivity. Results similar to panels C and D were obtained from 7 of 7 growth cones.

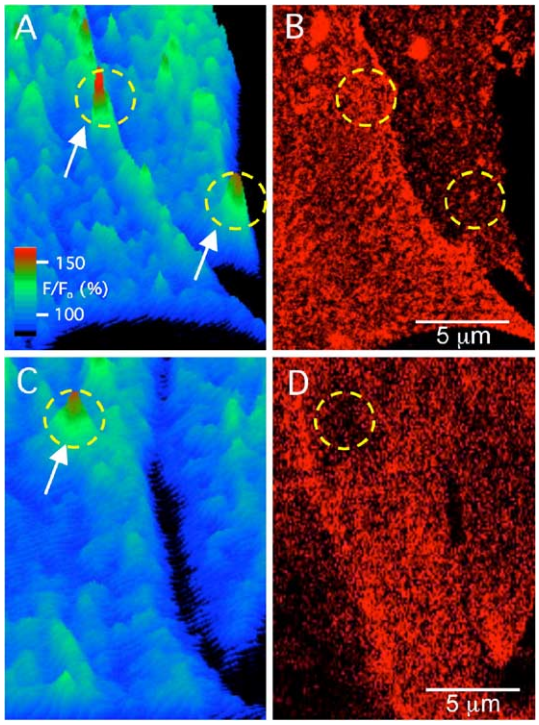

Fig. 10. Cyclosporin A suppresses the local reduction of pFAK immunoreactivity by LFTs. (A) Surface plot of fluo-4 fluorescence in two fibroblasts in the presence of 10 nM cyclosporin A, each of which generated a localized transient during the period of imaging (arrows). (B) The culture was fixed 5 min after imaging, and the same fibroblasts were stained for pFAK. There was no detectable reduction in pFAK immunoreactivity at the site of LFT generation compared to non-LFT generating sites in the same cell. The locations of the LFTs are indicated by yellow dashed circles. Similar results were obtained from 5 of 5 cells. (C) Surface plot of fluo-4 fluorescence in another fibroblast in the absence of cyclosporin A (control), which generated a LFT (arrow). (D) The culture was fixed 5 min after imaging the LFT and stained for pFAK. The site of LFT generation corresponds to a localized reduction in pFAK immunoreactivity.

Discussion

We describe a class of spontaneous, spatially discrete Ca^{2+} transients (LLTs) that are generated in the lamellipodia of neuronal growth cones. Second messengers such as Ca^{2+} can function on a microdomain scale (Goldberg et al., 2003). Although the generation of a messenger from a point source is limited in the range of its effects by diffusion, buffering, and uptake, sufficiently high local concentrations achieve significant functions. We find that LLTs cause reduction of pFAK-IR and deadhesion of growth cones evaluated by IRM. Although the pharmacological profile of LLTs is similar to that for growth cone and filopodial transients, indicating a potentially common mechanism of generation, LLTs are more frequent, faster, and more spatially compact than growth cone Ca^{2+} transients (Gu and Spitzer, 1995; Gomez and Spitzer, 1999) but are less frequent and slower than filopodial transients (Gomez et al., 2001). For each class of Ca^{2+} transient, the frequency is regulated by the substrate upon which the cells are plated, and some substrates are more effective in generating one class of transient than another. Different combinations of integrin heterodimers with distinct regional localizations may have distinct capabilities for generating classes of transients on different substrates.

We report a similar class of spontaneous, localized Ca^{2+} transients (LFTs) that are generated in fibroblasts. LFTs also stimulate loss of pFAK-IR and deadhesion of fibroblasts from their substrate, assessed by IRM, although they are pharmacologically distinct from LLTs. These findings are paralleled by observations that Ca^{2+} spikes in U87 astrocytoma cells, generated by another mechanism, are temporally correlated with disassembly of focal adhesions visualized by imaging green fluorescent protein-tagged FAK (Giannone et al., 2002, 2004). Thus, a common function may be achieved by Ca^{2+} transients generated by different pathways. Consistent with this view, *Xenopus* growth cone and myocyte Ca^{2+} transients are generated by different mechanisms (Gu and Spitzer, 1995; Ferrari et al., 1996, 1998), but both regulate assembly of the cytoskeleton.

Although the formation of focal contacts has been the object of intensive investigation, analysis of the removal of focal contacts has received less attention. Cells cultured from FAK knockout mice (Ilic et al., 1995) contain an abundance of focal contacts but do not move or send out processes, demonstrating the importance of FAK in focal contact turnover and implying that turnover of contacts enables motility. Some of the functions ascribed to pFAK may be carried out by molecules downstream of pFAK activation such as the tyrosine kinase Src (Schlaepfer and Hunter, 1998). Nevertheless, these mechanisms are still indirectly dependent upon pFAK activation. Our results suggest that Ca^{2+} transients act in parallel with pFAK to remove focal contacts. The difference between focal contact formation and removal is expected to affect growth cone and fibroblast traction. However, differences in the rates of axon extension in the presence and absence of Ca^{2+} are influenced by other factors as well, such as the cytoskeleton (Lautermilch and Spitzer, 2000).

Several models have been proposed describing a balance of forces that regulate assembly and disassembly of the focal complex. The phosphorylation state of proteins at the focal complex governed by the activities of kinases such as FAK appears to be critical. Studies of neutrophil migration by Maxfield and colleagues led them to propose that transient global increases in intracellular Ca^{2+} are required for local release of the rear uropod from attachment sites (Marks and Maxfield, 1990; Hendey and Maxfield, 1993; Lawson and Maxfield, 1995). Increases in intracellular Ca^{2+} that propagate throughout cultured U87 astrocytoma cells have been shown to stimulate dissolution of focal adhesions (Giannone et al., 2002, 2004). The present results, demonstrating highly localized elevations of intracellular Ca^{2+} and corresponding deadhesion, are consistent with these findings and extend them to a smaller scale.

What is the mechanism by which these local Ca^{2+} transients reduce pFAK-IR and stimulate deadhesion? Our results implicate the Ca^{2+}-dependent phosphatase calcineurin as part of the signal transduction pathway. Because calcineurin is a serine–threonine phosphatase, it cannot be directly responsible for the decrease in immunoreactivity of tyrosine-phosphorylated pFAK. Ca^{2+} transients in filopodia activate the Ca^{2+}-dependent protease calpain, which generates repulsive growth cone turning (Robles et al., 2003). Because active calpain alters the balance between tyrosine kinase and phosphatase activities in filopodia that results in a net decrease in tyrosine phosphorylation, it may contribute to reduction of pFAK-IR in growth cones. Calpain has been shown to regulate focal complex disassembly in fibroblasts (Bhatt et al., 2002). Given the direct interaction of FAK with paxillin (Schlaepfer et al., 1999), and its role in integrating and processing adhesion- and growth factor-related signals (Turner, 2000), reduction in paxillin binding could lead to dissociation from FAK and breakdown of focal adhesions (Bertolucci et al., 2005). Additionally, the small GTP-binding protein Rho is known to contribute to focal complex formation, and high activity stabilizes the complex against removal. pFAK is required for the transient decrease in Rho activity seen in motile cells with rapid focal complex turnover; thus, removal may be the result of Rho inhibition by pFAK (Ren et al., 2000). Regulation of focal complex dynamics is clearly multifactorial, and further work will be needed to identify all the components of the regulatory pathways.

Acknowledgments

This work was supported by NRSA NS41701 to MWC and NIH NINDS NS 15918 to NCS. We thank the members of our laboratory for discussions and Laura Borodinsky, Kurt Marek, and Cory Root for their comments on the manuscript.

Appendix A. Supplementary data

Supplementary data associated with this article can be found, in the online version, at doi:10.1016/j.ydbio.2005.09.006.

References

Balaban, N.Q., Schwarz, U.S., Riveline, D., Goichberg, P., Tzur, G., Sabanay, I., Mahalu, D., Safran, S., Bershadsky, A., Addadi, L., Geiger, B., 2001. Force and focal adhesion assembly: a close relationship studied using elastic micropatterned substrates. Nat. Cell Biol. 3, 466–472.

Bence-Hanulec, K.K., Marshall, J., Blair, L.A.C., 2000. Potentiation of neuronal L calcium channels by IGF-1 requires phosphorylation of the α_1 subunit on a specific tyrosine residue. Neuron 27, 121–131.

Bertolucci, C.M., Guibao, C.D., Zheng, J., 2005. Structural features of the focal adhesion kinase-paxillin complex give insight into the dynamics of focal adhesion assembly. Protein Sci. 14, 644–652.

Bhatt, A., Kaverina, I., Otey, C., Huttenlocher, A., 2002. Regulation of focal complex composition and disassembly by the calcium-dependent protease calpain. J. Cell Sci. 11, 3415–3425.

Bian, J.H., Ghosh, T.K., Wang, J.C., Gill, D.L., 1991. Identification of intracellular calcium pools. Selective modification by thapsigargin. J. Biol. Chem. 266, 8801–8806.

Bonhoeffer, T., Yuste, R., 2002. Spine motility: phenomenology, mechanisms, and function. Neuron 35, 1019–1027.

Calabrese, B., Tabarean, I.V., Juranka, P., Morris, C.E., 2002. Mechanosensitivity of N-type calcium channel currents. Biophys. J. 83, 2560–2574.

Calalb, M.B., Polte, T.R., Hanks, S.K., 1995. Tyrosine phosphorylation of focal adhesion kinase at sites in the catalytic domain regulates kinase activity: a role for Src family kinases. Mol. Cell. Biol. 15, 954–963.

Chakrabarti, R., Chang, J.Y., Erickson, K.L., 1995. T cell receptor-mediated Ca^{2+} signaling: release and influx are independent events linked to different Ca^{2+} entry pathways in the plasma membrane. J. Cell. Biochem. 58, 344–359.

Chang, H.Y., Takei, K., Sydor, A.M., Born, T., Rusnak, F., Jay, D.G., 1995. Asymmetric retraction of growth cone filopodia following focal inactivation of calcineurin. Nature 376, 686–690.

Cheng, H., Lederer, W.J., Cannell, M.B., 1993. Calcium sparks: elementary events underlying excitation-contraction coupling in heart muscle. Science 262, 740–744.

Conklin, M.W., Ahern, C.A., Vallejo, P., Sorrentino, V., Takeshima, H., Coronado, R., 2000. Comparison of Ca^{2+} sparks produced independently by two ryanodine receptor isoforms (type 1 or type 3). Biophys. J. 78, 1777–1785.

Danker, K., Gabriel, B., Heidrich, C., Reutter, W., 1998. Focal adhesion kinase pp125FAK and the beta 1 integrin subunit are constitutively complexed in HaCaT cells. Exp. Cell Res. 239, 326–331.

Davies, P.F., Robotewskyj, A., Griem, M.L., 1993. Endothelial cell adhesion in real time. Measurements in vitro by tandem scanning confocal image analysis. J. Clin. Invest. 91, 2640–2652.

Drazba, J., Liljelund, P., Smith, C., Payne, R., Lemmon, V., 1997. Growth cone interactions with purified cell and substrate adhesion molecules visualized by interference reflection microscopy. Dev. Brain Res. 100, 183–197.

Ferrari, M.B., Rohrbough, J.C., Spitzer, N.C., 1996. Spontaneous calcium transients regulate myofibrillogenesis in embryonic *Xenopus* myocytes. Dev. Biol. 178, 484–497.

Ferrari, M.B., Ribbeck, K., Hagler, D.J., Spitzer Jr., N.C., 1998. A calcium signaling cascade essential for myosin thick filament assembly in *Xenopus* myocytes. J. Cell Biol. 141, 1349–1356.

Geiger, B., Bershadsky, A., 2001. Assembly and mechanosensory function of focal contacts. Curr. Opin. Cell Biol. 5, 584–592.

Giannone, G., Ronde, P., Gaire, M., Haiech, J., Takeda, K., 2002. Calcium oscillations trigger focal adhesion disassembly in human U87 astrocytoma cells. J. Biol. Chem. 277, 26364–26371.

Giannone, G., Ronde, P., Gaire, M., Beaudouin, J., Haiech, J., Ellenberg, J., Takeda, K., 2004. Calcium rises locally trigger focal adhesion disassembly and enhance residency of focal adhesion kinase at focal adhesions. J. Biol. Chem. 279, 28715–28723.

Goldberg, J.H., Tamas, G., Aronov, D., Yuste, R., 2003. Calcium microdomains in aspiny dendrites. Neuron 40, 807–821.

Gomez, T.M., Spitzer, N.C., 1999. In vivo regulation of axon extension and pathfinding by growth-cone calcium transients. Nature 397, 350–355.

Gomez, T.M., Roche, F.K., Letourneau, P.C., 1996. Chick sensory neuronal growth cones distinguish fibronectin from laminin by making substratum contacts that resemble focal contacts. J. Neurobiol. 29, 18–34.

Gomez, T.M., Robles, E., Poo, M.M., Spitzer, N.C., 2001. Filopodial calcium transients promote substrate-dependent growth cone turning. Science 291, 1983–1987.

Gu, X., Spitzer, N.C., 1995. Distinct aspects of neuronal differentiation encoded by frequency of spontaneous Ca^{2+} transients. Nature 375, 784–787.

Hendey, B., Maxfield, F.R., 1993. Regulation of neutrophil motility and adhesion by intracellular calcium transients. Blood Cells 19, 143–161.

Hendey, B., Klee, C.B., Maxfield, F.R., 1992. Inhibition of neutrophil chemokinesis on vitronectin by inhibitors of calcineurin. Science 258, 296–299.

Ilic, D., Furuta, Y., Kanazawa, S., Tekeda, N., Sobue, K., Nakatsuji, N., Nomura, S., Fujimoto, J., Okada, M., Yamamoto, T., Alzawa, S., 1995. Reduced cell motility and enhanced focal adhesion contact formation in cells from FAK-deficient mice. Nature 377, 539–543.

Ingber, D., 2003. Mechanosensation through integrins: cells act locally but think globally. Proc. Natl. Acad. Sci. U. S. A. 100, 1472–1474.

Izzard, C.S., Lochner, L.R., 1980. Formation of cell-to-substrate contacts during fibroblast motility: an interference-reflexion study. J. Cell Sci. 42, 81–116.

Johnson, J.D., Chang, J.P., 2000. Novel, thapsigargin-insensitive intracellular Ca2+ stores control growth hormone release from goldfish pituitary cells. Mol. Cell. Endocrinol. 165, 139–150.

Koizumi, S., Bootman, M.D., Bobanovic, L.K., Schell, M.J., Berridge, M.J., Lipp, P., 1999. Characterization of elementary Ca^{2+} release signals in NGF-differentiated PC12 cells and hippocampal neurons. Neuron 22, 125–137.

Komuro, H., Rakic, P., 1996. Intracellular Ca^{2+} fluctuations modulate the rate of neuronal migration. Neuron 17, 275–285.

Kornberg, L., Earp, H.S., Parsons, J.T., Schaller, M., Juliano, R.L., 1992. Cell adhesion or integrin clustering increases phosphorylation of a focal adhesion-associated tyrosine kinase. J. Biol. Chem. 267, 23439–23442.

Kyle, E., Neckers, L., Takimoto, C., Curt, G., Bergan, R., 1997. Genistein-induced apoptosis of prostate cancer cells is preceded by a specific decrease in focal adhesion kinase activity. Mol. Pharmacol. 51, 193–200.

Lauffenburger, D.A., Horwitz, A.F., 1996. Cell migration: a physically integrated molecular process. Cell 84, 359–369.

Lautermilch, N.J., Spitzer, N.C., 2000. Regulation of calcineurin by growth cone calcium waves controls neurite extension. J. Neurosci. 20, 315–325.

Lawson, M.A., Maxfield, F.R., 1995. Ca^{2+}- and calcineurin-dependent recycling of an integrin to the front of migrating neutrophils. Nature 377, 75–79.

Lee, J., Jacobson, K., 1997. The composition and dynamics of cell-substratum adhesions in locomoting fish keratocytes. J. Cell Sci. 110, 2833–2844.

Marks, P.W., Maxfield, F.R., 1990. Transient increases in cytosolic free calcium appear to be required for the migration of adherent human neutrophils. J. Cell Biol. 110, 43–52.

Ming, G.L., Wong, S.T., Henley, J., Yuan, X.B., Song, H.J., Spitzer, N.C., Poo, M.M., 2002. Adaptation in the chemotactic guidance of nerve growth cones. Nature 417, 411–418.

Plump, A.S., Erskine, L., Sabatier, C., Brose, K., Epstein, C.J., Goodman, C.S., Mason, C.A., Tessier-Lavigne, M., 2002. Slit1 and Slit2 cooperate to prevent premature midline crossing of retinal axons in the mouse visual system. Neuron 33, 219–232.

Ren, X.D., Kiosses, W.B., Sieg, D.J., Otey, C.A., Schlaepfer, D.D., Schwartz, M.A., 2000. Focal adhesion kinase suppresses Rho activity to promote focal adhesion turnover. J. Cell Sci. 113, 3673–3678.

Ribera, A.B., Spitzer, N.C., 1989. A critical period of transcription required for differentiation of the action potential of spinal neurons. Neuron 2, 1055–1062.

Robles, E., Huttenlocher, A., Gomez, T.M., 2003. Filopodial calcium transients regulate growth cone motility and guidance through local activation of calpain. Neuron 38, 597–609.

Schaller, M.D., 2001. Biochemical signals and biological responses elicited by the focal adhesion kinase. Biochim. Biophys. Acta 1540, 1–21.

Schaller, M.D., Hildebrand, J.D., Shannon, J.D., Fox, J.W., Vines, R.R., Parsons, J.T., 1994. Autophosphorylation of the focal adhesion kinase, pp125FAK, directs SH2-dependent binding of pp60src. Mol. Cell. Biol. 14, 1680–1688.

Scherberich, A., Campos-Toimil, M., Ronde, P., Takeda, K., Beretz, A., 2000. Migration of human vascular smooth muscle cells involves serum-dependent repeated cytosolic calcium transients. J. Cell Sci. 113, 653–662.

Schlaepfer, D.D., Hunter, T., 1998. Integrin signalling and tyrosine phosphorylation: just the FAKs? Trends Cell Biol. 8, 151–157.

Schlaepfer, D.D., Hauck, C.R., Sieg, D.J., 1999. Signaling through focal adhesion kinase. Prog. Biophys. Mol. Biol. 71, 435–478.

Sieg, D.J., Hauck, C.R., Schlaepfer, D.D., 1999. Required role of focal adhesion kinase (FAK) for integrin-stimulated cell migration. J. Cell Sci. 112, 2677–2691.

Singer, I.I., Kazazis, D.M., Scott, S., 1989. Scanning electron microscopy of focal contacts on the substratum attachment surface of fibroblasts adherent to fibronectin. J. Cell Sci. 93, 147–154.

Tang, F., Dent, E.W., Kalil, K., 2003. Spontaneous calcium transients in developing cortical neurons regulate axon outgrowth. J. Neurosci. 23, 927–936.

Tash, J.S., Krinks, M., Patel, J., Means, R.L., Klee, C.B., Means, A.R., 1988. Identification, characterization, and functional correlation of calmodulin-dependent protein phosphatase in sperm. J. Cell Biol. 106, 1625–1633.

Turner, C.E., 2000. Paxillin and focal adhesion signalling. Nat. Cell Biol. 2, E231–E236.

Verschueren, H., 1985. Interference reflection microscopy in cell biology: methodology and applications. J. Cell Sci. 75, 279–301.

Wu, X., Davis, G.E., Meininger, G.A., Wilson, E., Davis, M.J., 2001. Regulation of the L-Type calcium channel by $\alpha_5\beta_1$ integrin requires signaling between focal adhesion proteins. J. Biol. Chem. 276, 30285–30292.

Yao, Y., Choi, J., Parker, I., 1995. Quantal puffs of intracellular Ca^{2+} evoked by inositol trisphosphate in *Xenopus* oocytes. J. Physiol. 482, 533–553.

Zemir, E., Geiger, B., 2001. Molecular complexity and dynamics of cell-matrix adhesions. J. Cell Sci. 114, 3583–3590.

Zheng, J.Q., 2000. Turning of nerve growth cones induced by localized increases in intracellular calcium ions. Nature 403, 89–93.